Applied Thermal Engineering 63 (2014) 227–233

Contents lists available at ScienceDirect

Applied Thermal Engineering

journal homepage: www.elsevier.com/locate/apthermeng

Operation characteristics of air-cooled proton exchange membrane fuel cell stacks under ambient pressure

Houchang Pei [a], Jun Shen [a], Yonghua Cai [b], Zhengkai Tu [b,*], Zhongmin Wan [a,c], Zhichun Liu [a,**], Wei Liu [a]

[a] School of Energy and Power Engineering, Huazhong University of Science and, Technology, Wuhan 430074, China
[b] State Key Laboratory of Advanced Technology for Materials Synthesis and Processing, Wuhan University of Technology, Wuhan 430070, China
[c] College of Information Engineering, Hunan Institute of Science and Technology, Yueyang 414006, China

HIGHLIGHTS

- Effect of cell order on air-cooled stack performance can be neglected.
- Thickness and PTFE content in GDL are founded with optimization values.
- Temperature distribution should remain at proper range.

ARTICLE INFO

Article history:
Received 19 June 2013
Accepted 6 November 2013
Available online 15 November 2013

Keywords:
Proton exchange membrane fuel cell (PEMFC)
Gas diffusion layer (GDL)
Polytetrafluoroethylene (PTFE) content
Air-cooled

ABSTRACT

Air-cooled proton exchange membrane fuel cells (PEMFC) simplify the traditional cooling and air supply system. Three air-cooled stacks are assembled with different cells to investigate the effect of the polytetrafluoroethylene (PTFE) content in the gas diffusion layer (GDL), air flow rate, as well as the stack temperature on the stack performance. The results show that GDL with appropriate thickness and PTFE content can optimize the stack operation performance. The effect of the cell order on its performance can be neglected. A thermal equilibrium resulting from the heat generation and loss in the stack is achieved near the ambient temperature at low current density of 150 mA cm^{-2}. The output power increases with the increase of air flow rate. However, when the air flow rate exceed 44.7 L min^{-1} or the stack temperature is higher than 65 °C, the stack performance decreases.

1. Introduction

Proton exchange membrane fuel cell (PEMFC) is an energy conversion device that directly converts the chemical energy stored in hydrogen and oxidant into electrical energy. The PEMFC is a promising alternative to batteries as a power supply for consumer electronics, sensors and medical devices, and it is considered to be the first choice for the 21st century clean, efficient power generation technology [1–8]. The efficiency of conventional PEMFC stack is about 50% and the rest of the energy is released in the form of heat [9–13]. The PEMFC stack temperature would increase rapidly if the generated heat cannot be efficiently removed from the stack continuously. The increased temperature of the cell makes the membrane dehydrated and lowers the proton conductivity of the membrane, causing poor performance of the fuel cell and eventually leading to irreversible damages. Thus adequate attention must be paid to the design of an efficient cooling system for PEMFC stack [14–18]. In order to achieve higher efficiency, the membrane of PEMFC should be kept at a certain hydrated level to facilitate proton transport and the conventional PEMFC stack should have a special humidification system to keep the reaction gas at certain humidity. Consequently, additional auxiliary system must be applied to the PEMFC stack, which increases the complexity of PEMFC system and limits its application as a portable power system. Air-cooled PEMFC stack could simplify the cooling system, humidification and air compressor or pump system. Special channel has been designed to combine air supply and cooling system to make its applications more convenient in the field of portable power systems [19,20].

Extensive research efforts, both numerical modeling [21–25] and experimental investigations [26–31], have been conducted on air-cooled PEMFC stack. Ying [21] investigated the effect of

* Corresponding author. Fax: +86 27 87879468.
** Corresponding author. Fax: +86 27 87540724.
E-mail addresses: tzklq@whut.edu.cn (Z. Tu), zcliu@hust.edu.cn (Z. Liu).

1359-4311/$ – see front matter © 2013 Elsevier Ltd. All rights reserved.
http://dx.doi.org/10.1016/j.applthermaleng.2013.11.012

channel configuration on air-breathing fuel cell performance, and the results showed that an optimal performance could be obtained in the cell with cathode channel width of 3.0 mm (open ratio of 75.9%). Schmitz et al. [26,27] investigated an air-breathing PEM fuel cell and demonstrated that the inlet size of the cathode and the wetting properties of the GDL have an important effect on stack performance. It was revealed that the cathode flow with the 80% opening ratio is the optimal value. The hydrophilic or hydrophobic property of GDLs has little effect on stack performance. Finally, the authors gave two design rules for air-breathing PEMFCs. Ous [28] studied the water management in an air-breathing PEMFC. Their result showed that the gas stoichiometry had little effect on the water removal from the channels. Hottinen [29] studied the cold-start behavior of free-breathing PEMFC. They found that the freezing of product water inside the cell would damage the stack irreversibly at low temperature. The free-breathing PEMFC stack can start successfully at −5 °C when the cell was initially dry. Air-breathing PEM fuel cell stack has low power density and poor power output, which limits its application. In contrast, air-cooled PEM fuel cell stack usually uses an air fan at the edge of the open cathode manifolds to force air flow which guarantees sufficient oxidant supply and cools the stack, resulting in a wide power output range from 300 W to 4 kW. Wu [30] designed an air-cooled single PEM fuel cell and a 5-cell air-cooled stack to investigate the effects of critical operating conditions on the output performance. It was indicated that the cell temperature and hydrogen humidifier play important roles in reducing the fuel cell ohmic resistance. It was also observed that a hydrophilic treatment of the cathode flow field channels could improve the water management. Rosa [31] studied the influence of different operating parameters on the performance of the stack in an 8-cell air-cooled PEM fuel cell stack. They concluded that the stack performance could be significantly increased while operated with forced air convection instead of natural convection and the stack performance was practically not affected by hydrogen partial pressure. Sohn [32] analyzed the effect of relative humidity, the temperature of the stack, the utility ratio of the reactant gas on the performance of an air-cooling PEMFC. Kim [33] studied the effects of the cathode channel size and operating conditions on the performance of the air-blowing PEMFC. It was found that the output of the PEMFC stack could be improved with the decrease of the cathode channel size at the normal operating temperature. Massive flooding limits the decrease in the cathode channel size. Transition current density between the humidification and the flooding region decreased with decreasing cathode channel size and operating temperature.

Although both air-breathing and air-cooled PEM fuel cells have been studied, little attention has been devoted to the systematic development of cell components characteristic and operating conditions, such as GDL characteristics, air flow rate and stack temperature. In this work, a study of several crucial parameters, such as the GDL thickness, PTFE content of GDL, air flow rate, and cell temperature, was carried out on the performance of an air-cooled PEM fuel cell stack, and the results can provide in situ diagnostic data for the maintenance of stable power generation station equipped with air-cooled PEM fuel stack.

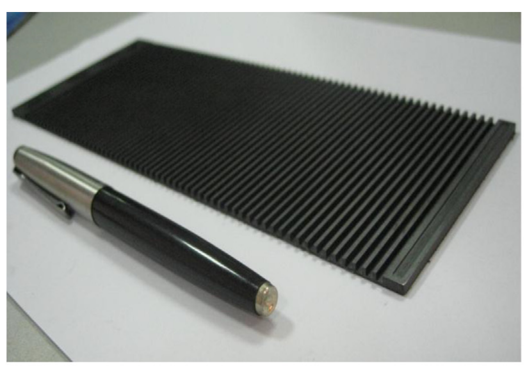

(a)Cathode flow field of cell (width: 2.0 mm; depth: 1.8mm; land: 1.2 mm, length of channel: 80mm.)

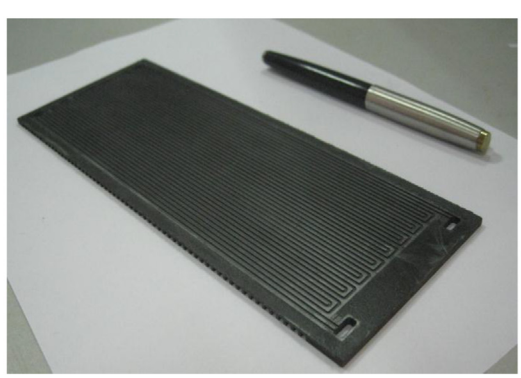

(b) Anode flow field of cell (2-channel serpentine flow field)

Fig. 1. Graphite bipolar-plate of air-cooling stack.

2. Experimental system

2.1. The experimental materials

Fig. 1(a) shows the structure of the flow field used at the cathode, which consists of several parallel straight channels. Each channel is 2.0 mm in width, 1.8 mm in depth and the land is 1.2 mm. For the anode plate, a 2-channel serpentine flow field (1.0 mm in width and 0.4 mm in depth with a land with of 1.0 mm) is designed as shown in Fig. 1(b). The membrane electrode assembly (MEA) active area is 100 cm^2 prepared by WHUT technology with Nafion® 211 membrane and TORY carbon paper as gas diffusion layer (GDL). The stack system includes an additional air fan (SUNON PMD2409PMB1-A) controlled by a rheostat. In this study, the cell and stack are all operated in a vertical position. The dry air flows from upper to bottom and its flow rate in the cathode flow field is adjusted by changing the fan voltage, as shown in Fig. 2.

2.2. Air-cooled PEM fuel cell stack test

The experiments were performed on a commercial fuel cell test station (FCATS G500) purchased from Canadian Greenlight Company, which was equipped with mass flow controllers, reactant gas humidification, dew point temperature, and a programmable electric load. FCATS G500 supplied hydrogen to the stack while the air supply was an accessorial fan controlled by a rheostat. To avoid the damage of MEA, the load was set to be automatically disconnected once the minimum voltage of any signal cell drops to 0.2 V or the voltage decreases rapidly in 4 s. The polarization curves were measured by scanning the current density ranging from 0 to 800 mA cm^{-2}. Each step was applied for 5 min and the steady-state individual cell voltage, output power, cell temperature and flow rate were then recorded automatically. The sketch of the test system is shown in Fig. 3

3. Results and discussion

3.1. Effect of GDL thickness on the stack performance

To keep high performance of the stack, the membrane should have sufficient water and the stack should be supplied with enough reactant gas [34]. He [35] developed a fractal model to predict the permeability and liquid water relative permeability of the GDL. The results revealed that the water relative permeability in the hydrophobic case is much higher than that in the hydrophilic case. A hydrophobic GDL is good for liquid water removal from the cathode. LaManna [36] investigated the effect of GDL thickness on the effective water vapor diffusion coefficient. It was realized that thickness had a negligible influence on the effective diffusion coefficient measurement as expected since thickness is accounted for diffusion calculations. Chun [37] performed numerical modeling and experimental study of the influence of GDL properties on performance in a PEMFC. It was concluded that the cell performance decreased with the increase in GDL thickness, attributed to the rapid liquid water saturation and the decreased oxygen concentration near the catalyst layer with increasing GDL thickness. In an air-cooled stack, thinner GDL is preferred for water and gas transfer in principle. However, it can also result in rapid water evaporation in membranes and less physical support to the MEA [38]. In contrast, thicker GDL can prevent water evaporation from the GDL surface and is good for retaining water in the air-cooled PEMFC stack. However, too thick GDL requires much longer diffusion time for oxidant from gas channel to catalyst layer, which in turn leads to the decrease of the stack performance. Thus, an optimum GDL thickness is very important for air-cooled PEMFC stack.

Fig. 2. Structure of the air-cooling stack.

3.1.1. Performance of the stacks with different thicknesses of GDL

An 8-cell stack was fabricated to investigate the effects of GDL thickness on stack performance. The MEAs of the stack were prepared with different thickness of GDL (PTFE content 30%) and numbered as shown in Table 1. Data were obtained at room temperature (20 °C), the stoichiometry of the dry hydrogen was 1.5, and the flow rate in the cathode was 20.0 L min^{-1}. Fig. 4 shows the voltage of each single cell in the stack at different current densities. It can be observed that voltages of cell #5 and #2 were higher than other cells and the lowest voltage was observed in cell #8 at different current densities. As all the cells were operated in the same operating condition, the GDL thickness of 0.6 mm in cell #5 and #2 should be the optimal value.

3.1.2. Changing the cell order

In order to minimize the performance difference due to different order of the single cells, an 8-cell stack was reassembled to investigate the performance. Table 2 showed the new serial number of each single cell. GDL with thickness of 0.6 mm was used in cell #1 and #8, and 1.0 mm GDL thickness was used in cell 5 in the reassembled stack. Compared with Fig. 4, as shown in Fig. 5, cells with 0.6 mm GDL remained the best performance, and cells with 1.0 mm GDL still showed the worst performance in the reassembled stack. Moreover, cells fabricated with GDL in other thicknesses (0.2 mm, 0.4 mm, and 0.8 mm) were also operated at the same voltages under different current densities. Thus, it can be concluded that the voltage of the same single cell has little relationship with its different order in the stack. Fig. 6 shows the relationships between the cell performance and GDL thickness. With the increase in the GDL thickness, the performance of the cell improves until it reached its optimal value of 0.6 mm, and then the operation voltage drops. The main reason is that thinner GDL leads to membrane dehydration due to the enhanced water evaporation with the air flow. GDL with thickness of 0.6 mm could maintain the water balance in the membrane, and catalyst layer will be flooded when the thickness exceeds 0.6 mm.

As a consequence, thinner GDL would increase the contact resistance between the GDL and the bipolar plates, leading to the decreased performance. Contrarily, coupled effect of the poor gas diffusion and water removal ability would appear at the excess thickness of GDL.

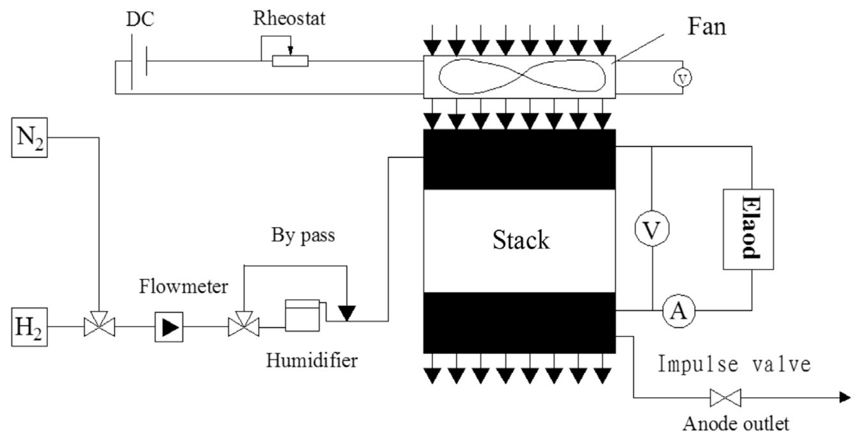

Fig. 3. Sketch of the test system.

Table 1
Serial number of single cell GDL.

MEA serial number	1#	2#	3#	4#	5#	6#	7#	8#
GDL Thickness (mm)	0.2	0.6	0.2	0.8	0.6	0.4	0.8	1.0

Table 2
Serial number of single cell GDL of reassembly stack.

MEA serial number	1#	2#	3#	4#	5#	6#	7#	8#
GDL thickness (mm)	0.6	0.2	0.4	0.8	1.0	0.2	0.8	0.6

3.2. Effect of PTFE content of GDL on stack performance

Currently, the GDL was treated with polytetrafluoroethylene (PTFE) to enhance water and gas management [39–41]. GDL with proper PTFE content helps remove the water when the cells are under flooding conditions. A 10-cell air-cooled stack with the same flow field and GDL thickness (0.6 mm) was fabricated to investigate the effect of PTFE content in GDL on the cell performance. Each MEA with different PTFE content was numbered as shown in Table 3. To avoid the effect of the cell order in stack on the performance, GDL with different PTFE contents in single cell was placed symmetrically on the cycle circuit. Fig. 7 shows the voltages of each single cell in the stack at different current densities. It was clear that the voltages of cell #2 and #7 with the PTFE content of 40% were higher than other cells and cell #10 without hydrophobic disposal exhibited the lowest voltage value at different current densities. The difference between the maximal and minimum voltage in this stack increases with the increase in current density. The results revealed that elevated PTFE content in GDL could enhance the cell performance, especially at higher current densities where more water is generated and needs to be removed from the cell. Simultaneously, the voltage differences between the cells equipped with the same PTFE content in different positions were ±0.01 V, which could be also deduced in Figs. 4 and 5. Contrarily, the differences between the cells with different PTFE contents increased to 0.11 V at 600 mA cm^{-2}. Thus, PTFE content in GDL plays a very important role in cell performance of air-cooled PEM stack, and the cell order has negligible effects on the cell voltage. Fig. 8 showed the relationship between PTFE content of GDL and cell voltage. Cell voltage increased to the peak value while the content of PTFE in GDL increased to 40%. As the carbon paper was treated by PTFE, porous skeleton in the carbon paper can be covered, leading to the decrease of pore size. Therefore, higher PTFE content would reduce the porosity in GDL and the resistance for reaction gas spreading from gas channel to catalyst layer increased. Meanwhile, GDL

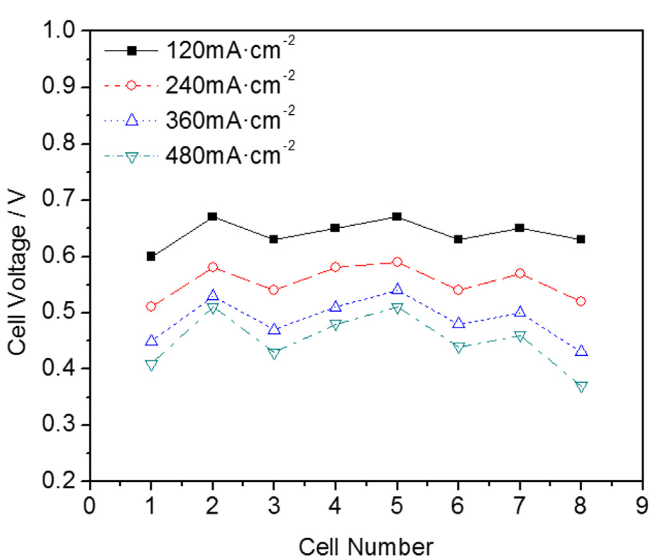

Fig. 4. Single cell voltage with different thicknesses of GDL.

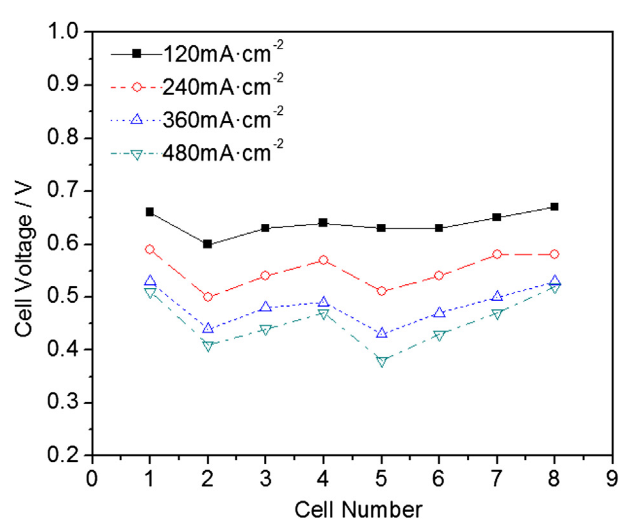

Fig. 5. Cell voltage of reassembly stack.

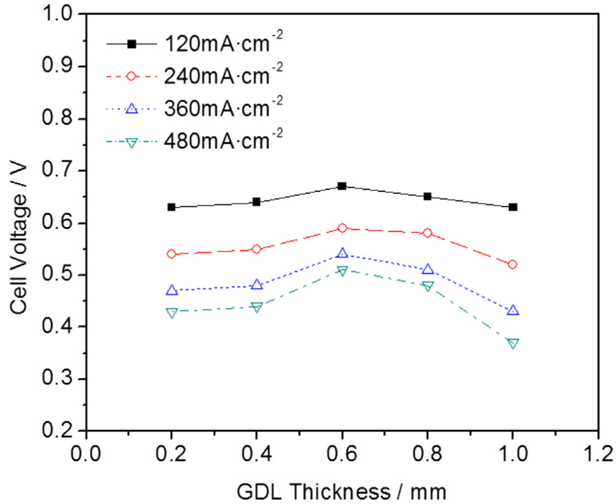

Fig. 6. Relationship between cell voltage and GDL thickness.

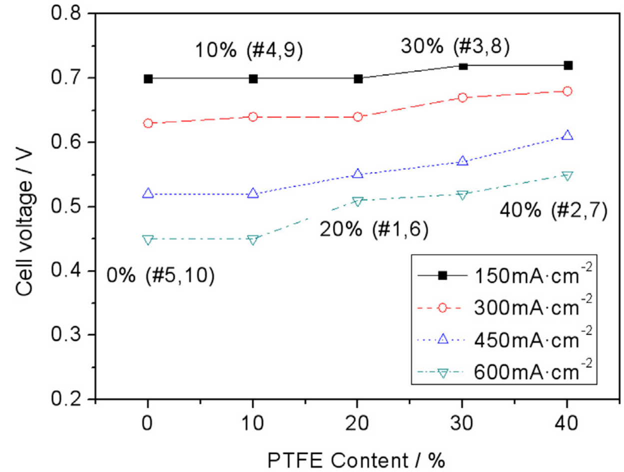

Fig. 8. Effect of PTFE content on stack performance.

Table 3
Serial number of GDL with different PTFE content.

Cell serial	1#	2#	3#	4#	5#	6#	7#	8#	9#	10#
PTFE content	20%	40%	30%	10%	0	20%	40%	30%	10%	0

treated with PTFE is hydrophobic that greatly affects the water management of the cell [42,43]. Both the PTFE content and porosity of GDL play an important role in stack performance. The porosity of GDL mainly affects the mass transfer performance, and the PTFE content of GDL affects water removal from catalyst to channel, predominantly [42,43]. To achieve good performance of the stack, PTFE content and porosity of GDL should be treated in an optimized value. As a result, water convection with the dry flow air was constrained and sufficient generated water was maintained near the membrane to enhance the proton conductivity.

3.3. *Effect of air flow rate on stack performance*

Air flow rate is a key parameter to the operation of an air-cooled stack. According to the results above, a 19-cell stack with the PTFE content of 40% and thickness of 0.6 mm in GDL was assembled to investigate the effect of air flow on stack performance. In the test, the hydrogen stoichiometry was 1.2 without humidification and the ambient temperature was 20 °C. Air flow was set as 27.0 L min^{-1}, 31.7 L min^{-1}, 35.3 L min^{-1}, 40.0 L min^{-1}, 41.7 L min^{-1}, 44.7 L min^{-1}, and 47.3 L min^{-1}. Fig. 9 shows the polarization curves of air-cooled stack at different air flow rates. The power density initially increases as the air flow rate increases, and reaches the peak value of 295 mW cm^{-2} when the current density is 600 mA cm^{-2} and the air flow rate is 44.7 L min^{-1}. Three regions were observed due to the effect of air flow rate. In the first region, the single cell voltage decreased rapidly with the air flow rate varied from 27.0 L min^{-1} to 31.7 L min^{-1}, and the stack became unstable as the current density increased to 350 mA cm^{-2}. In the second region, the maximum operated current density could reach 550 mA cm^{-2} when the air flow rate increased from 35.3 L min^{-1} to 41.7 L min^{-1}. The operated current density could reach 650 mA cm^{-2} when the air flow rate increased to 47.3 L min^{-1} in the third region. However, in the third zone, the maximum output power appeared at the air flow rate of 44.7 L min^{-1}, but not 47.3 L min^{-1}. The main reason is that water flooding is the dominant effect on the performance at low air flow rate and the generated water is not effectively removed from the membrane in this situation. With the increase in the air flow rate, the water removal ability improves and the stack could reach the maximum output power when the air flow is 44.7 L min^{-1}. However, excessive

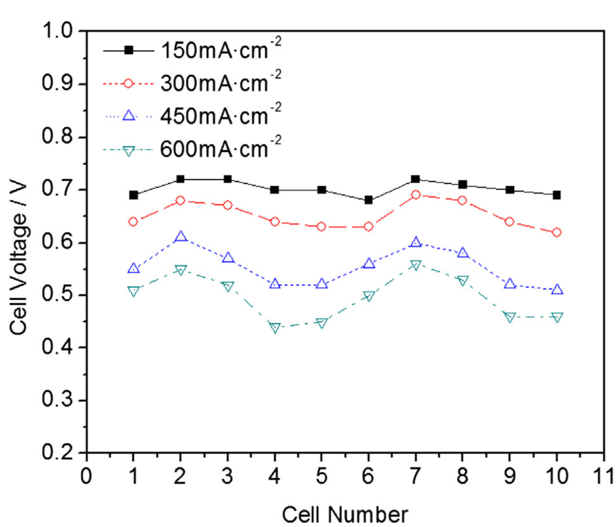

Fig. 7. Single cell voltage uniformity with different PTFE content.

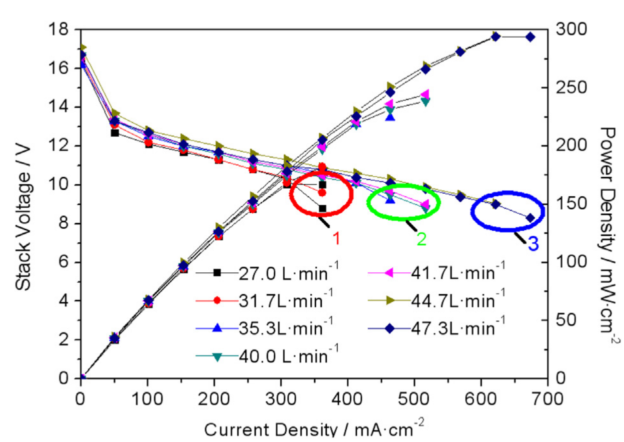

Fig. 9. Performance of stack at different air flow rates.

air flow rate causes water to evaporate from the membrane and results in membrane dehydration, leading to the decreased performance of the stack.

3.4. Effect of temperature on stack performance

The electrode reaction kinetics could be enhanced with the increase in operating temperature. On the other hand, the elevated temperature of the cell could cause membrane dehydration and eventually lead irreversible damage. Fig. 10(a) shows the variation of air-cooled temperature at different current densities and air flow rates. The stack temperature increases as the current density increases. It was also observed that the stack voltage became instable when the temperature was higher than 65 °C. The maximum power density of the stack appeared at the stack temperature of 65 °C in Fig. 9. Fig. 10(b) shows the current density of the stack as a function of air flow rate under different temperatures. The effect of the increased air flow rate on the stack temperature could be neglected at low current density, and the stack temperature began to decrease rapidly with increasing air flow rate, especially at high current density. The reason is that heat generated due to the electrochemical reaction is less at low current density and it can be easily removed by the air flow due to convection heat transfer. Accordingly, the stack performance would remain near ambient temperature. Heat generated in the cell and removed by the air flow was equal and heat balance could be achieved inside the stack at 65 °C. Accordingly, the stack reached its optimal operating state in this situation. With further increase in air flow rate, the air flow plays a dominated role in the stack temperature, and the stack temperature decreases rapidly at the elevated air flow rate, leading to reduced performance.

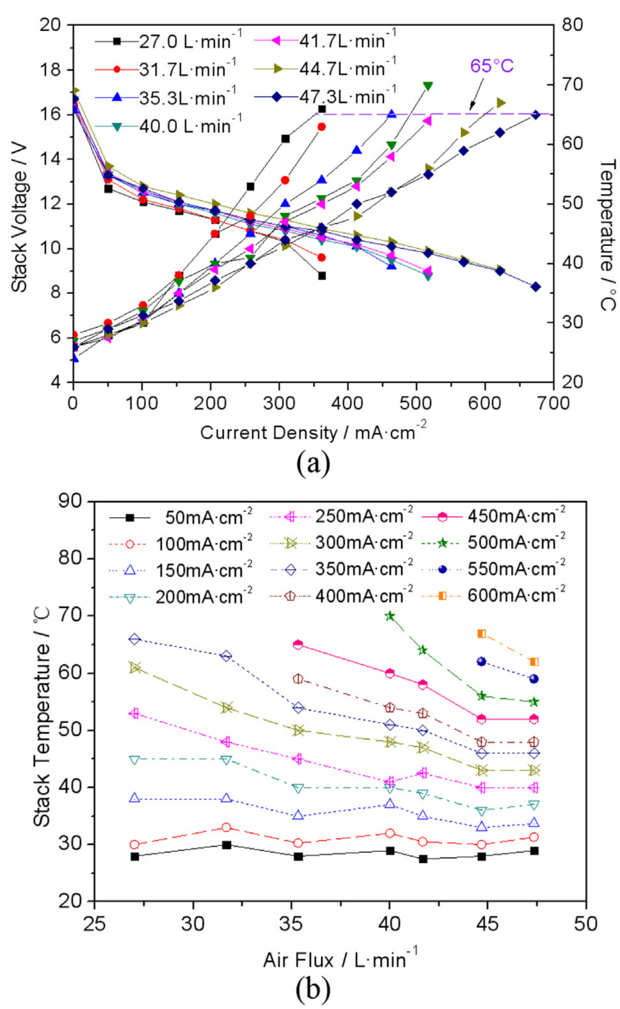

Fig. 10. Relations between current density and stack temperature.

4. Conclusions

Three air-cooled PEMFC stacks were developed and studied at several crucial operation conditions. The effects of the PTFE content in GDL, air flow rate and cell temperature on the performance were investigated in detail. The conclusions can be drawn as follows:

(1) Optimization of the thickness and PTFE content in GDL can improve the performance of the air-cooled stack, and the effect of the cell order on the performance can be neglected.
(2) Elevated air flow rate is helpful for the water management in the air-cooled stack. However, excess air flow rate would make significant water evaporation from the membrane, resulting in the membrane dehydration and the decreased performance of the stack.
(3) Heat generated in the stack and removed by the air flow reached the thermal balance at an optimal value near the ambient temperature at low current density. The stack temperature decreases rapidly at over-elevated air flow rate and results in decreased performance.

Acknowledgements

This work was financially supported by the Ministry of Science and Technology 863 Hi-Technology Research and Development Program of China (No. 2012AA110600), the National Science Foundation of China (Nos. 51036003 and 51376058), and the Fundamental Research Funds for the Central Universities (WUT: 2012IV084). The authors are grateful to Dr. Lingping, Zeng at Massachusetts Institute of Technology (MIT) for his discussion and language editing.

References

[1] S.W. Perng, H.W. Wu, Heat transfer in a PEMFC flow channel, Appl. Therm. Eng. 29 (2009) 3579–3594.
[2] U. Soupremanien, S.L. Person, M. Favre-Marinet, et al., Tools for designing the cooling system of a proton exchange membrane fuel cell, Appl. Therm. Eng. 40 (2012) 161–173.
[3] H.L. Tang, M. Pan, F. Wang, A mechanical durability comparison of various perfluorocarbon proton exchange membranes, J. Membr. Sci. 109 (2008) 2671–2678.
[4] H.C. Pei, Z.C. Liu, H. Zhang, et al., In situ measurement of temperature distribution in proton exchange membrane fuel cell I a hydrogen-air stack, J. Power Sources 22 (2013) 772–779.
[5] F. Wang, H.L. Tang, M. Pan, et al., Ex situ investigation of the proton exchange membrane chemical decomposition, Int. J. Hydrogen Energy 33 (2008) 2283–2288.
[6] E. Harikishan Reddy, S. Jayanti, Thermal management strategies for a 1 kWe stack of a high temperature proton exchange membrane fuel cell, Appl. Therm. Eng. 48 (2012) 465–475.
[7] J. Pan, H. Zhang, W. Chen, M. Pan, Nafion–zirconia nanocomposite membranes formed via in situ sol–gel process, Int. J. Hydrogen Energy 35 (2010) 2796–2801.
[8] K. Li, G.B. Ye, J.J. Pan, et al., Self-assembled Nafion®/metal oxide nanoparticles hybrid proton exchange membranes, J. Membr. Sci. 347 (2010) 26–31.
[9] Y. Yu, Z.K. Tu, H.N. Zhang, et al., Gravity effect on the performance of PEM fuel cell stack with different gas inlet/outlet positions, Int. J. Energy. Res. 36 (2012) 845–855.
[10] Z.K. Tu, H.N. Zhang, Z.P. Luo, et al., Evaluation of 5 kW proton exchange membrane fuel cell stack operated at 95 °C under ambient pressure, J. Power Sources 222 (2013) 277–281.
[11] Y. Wang, K.S. Chen, J. Mishler, et al., A review of polymer electrolyte membrane fuel cells: technology, applications, and needs on fundamental research, Appl. Energy 88 (2011) 981–1007.

[12] Z.M. Wan, J.H. Wan, J. Liu, et al., Water recovery and air humidification by condensing the moisture in the outlet gas of a proton exchange membrane fuel cell stack, Appl. Therm. Eng. 42 (2012) 173–178.
[13] S.G. Kandlikar, Z.J. Lu, Thermal management issues in a PEMFC stack – a brief review of current status, Appl. Therm. Eng. 29 (2009) 1276–1280.
[14] S. Pandiyan, K. Jayakumar, N. Rajalakshmi, et al., Thermal and electrical energy management in a PEMFC stack-An analytical approach, Int. J. Heat Mass Transfer 51 (2008) 469–473.
[15] E. Özden, I. Tolj, F. Barbir, Designing heat exchanger with variable surface area for passive cooling of PEM fuel cell, Appl. Therm. Eng. 51 (2013) 1339–1344.
[16] P.Y. Yi, L.F. Peng, X.M. Lai, et al., A novel design of wave-like PEMFC stack with undulate MEAs and perforated bipolar plates, Fuel Cells 10 (2010) 111–117.
[17] P.Y. Yi, L.F. Peng, X.M. Lai, et al., Investigation of sintered stainless steel fiber felt as gas diffusion layer in proton exchange membrane fuel cells, Int. J. Hydrogen Energy 37 (2012) 11334–11344.
[18] R. Cozzolino, S.P. Cicconardi, E. Galloni, et al., Theoretical and experimental investigations on thermal management of a PEMFC stack, Int. J. Hydrogen Energy 36 (2011) 8030–8037.
[19] A.R. Maher, A. Sadiq, Performance comparison between airflow-channel and ambient air-breathing PEM fuel cells using three-dimensional computational fluid dynamics models, Renew. Energy 34 (2009) 1812–1824.
[20] N. Karst, V. Faucheux, A. Martinent, et al., Innovative water management in micro air-breathing polymer electrolyte membrane fuel cells, J. Power Sources 195 (2010) 1156–1162.
[21] W. Ying, J. Ke, W.Y. Lee, et al., Effects of cathode channel configurations on the performance of an air-breathing PEMFC, Int. J. Hydrogen Energy 3 (2005) 1351–1361.
[22] W. Ying, Y.J. Sohn, W.Y. Lee, et al., Three-dimensional modeling and experimental investigation for an air-breathing polymer electrolyte membrane fuel cell (PEMFC), J. Power Sources 145 (2005) 563–571.
[23] W. Ying, T.H. Yang, W.Y. Lee, et al., Three-dimensional analysis for effect of channel configuration on the performance of a small air-breathing proton exchange membrane fuel cell (PEMFC), J. Power Sources 145 (2005) 572–581.
[24] R. O'Hayre, T. Fabian, S. Litster, et al., Engineering model of a passive planar air breathing fuel cell cathode, J. Power Sources 167 (2007) 118–129.
[25] R. Glises, D. Hissel, F. Harel, et al., New design of a PEM fuel cell air automatic climate control unit, J. Power Sources 150 (2005) 78–85.
[26] A. Schmitz, M. Tranitz, S. Wagner, et al., Planar self-breathing fuel cells, J. Power Sources 118 (2003) 162–171.
[27] A. Schmitz, M. Tranitz, S. Eccarius, et al., Influence of cathode opening size and wetting properties of diffusion layers on the performance of air-breathing PEMFCs, J. Power Sources 154 (2006) 437–447.
[28] T. Ous, C. Arcoumanis, The formation of water droplets in an air-breathing PEMFC, Int. J. Hydrogen Energy 34 (2009) 3476–3487.
[29] T. Hottinen, I. Himanen, P. Lund, Performance of planar free-breathing PEMFC at temperatures below freezing, J. Power Sources 138 (2004) 205–210.
[30] J.F. Wu, S. Galli, I. Lagana, et al., An air-cooled proton exchange membrane fuel cell with combined oxidant and coolant flow, J. Power Sources 188 (2009) 199–204.
[31] D.T. Santa Rosa, D.G. Pinto, V.S. Silva, et al., High performance PEMFC stack with open-cathode at ambient pressure and temperature conditions, Int. J. Hydrogen Energy 32 (2007) 4350–4357.
[32] Y.J. Sohn, G.G. Park, T.H. Yang, et al., Operating characteristics of an air-cooling PEMFC for portable applications, J. Power Sources 145 (2) (2005) 604–609.
[33] B. Kim, Y. Lee, A. Woo, et al., Effects of cathode channel size and operating conditions on the performance of air-blowing PEMFCs, Appl. Energy 111 (2013) 441–448.
[34] N. Djilali, D.M. Lu, Influence of heat transfer on gas and water transport in fuel cells, Int. J. Therm. Sci. 41 (2002) 29–40.
[35] G. He, Z. Zhao, P. Ming, et al., A fractal model for predicting permeability and liquid water relative permeability in the gas diffusion layer (GDL) of PEMFCs, J. Power Sources 163 (2) (2007) 846–852.
[36] J.M. LaManna, S.G. Kandlikar, Determination of effective water vapor diffusion coefficient in PEMFC gas diffusion layers, Int. J. Hydrogen Energy 36 (8) (2011) 5021–5029.
[37] J.H. Chun, K.T. Park, D.H. Jo, et al., Numerical modeling and experimental study of the influence of GDL properties on performance in a PEMFC, Int. J. Hydrogen Energy 36 (2011) 1837–1845.
[38] W. Dai, H.J. Wang, X.Z. Yuan, et al., Measurement of water transport rates across the gas diffusion layer in a PEM fuel cell, and the influence of PTFE content and micro-porous layer, J. Power Sources 188 (2009) 122–126.
[39] D. Bevers, R. Rogers, M.V. Bradke, Examination of the influence of PTFE coating on the properties of carbon paper in polymer electrolyte fuel cells, J. Power Sources 63 (1996) 193–201.
[40] L.R. Jordan, A.K. Shukla, T. Behrsing, et al., Diffusion layer parameters influencing optimal fuel cell performance, J. Power Sources 86 (2000) 250–254.
[41] G. Lin, T.V. Nguyen, A two-dimensional two-phase model of a PEM fuel cell, J. Electrochem. Soc. 152 (2005) A1942–A1948.
[42] G.G. Park, Y.J. Sohn, T.H. Yang, et al., Effect of PTFE contents in the gas diffusion media on the performance of PEMFC, J. Power Sources 131 (2004) 182–187.
[43] C. Lim, C.Y. Wang, Effects of hydrophobic polymer content in GDL on power performance of a PEM fuel cell, Electrochim. Acta 49 (2004) 4149–4156.